NASA Technical Paper 2816

1988

Computer-Aided Design Analysis of 57-mm, Angular-Contact, Cryogenic Turbopump Bearings

Elizabeth S. Armstrong
and Harold H. Coe

Lewis Research Center
Cleveland, Ohio

National Aeronautics
and Space Administration

Scientific and Technical Information Division

Summary

The space shuttle main engine (SSME) high-pressure oxygen turbopumps (HPOTP) have not experienced the service life required of them. This insufficiency has been due in part to the shortened life of the bearings. To improve the life of the existing turbopump bearings, an effort is being undertaken to investigate bearing modifications that could be retrofitted into the present bearing cavity. Several bearing parameters were optimized using the computer program SHABERTH, which performs a thermomechanical simulation of a load support system. The computer analysis showed that improved bearing performance is feasible if low friction coefficients can be attained. Bearing geometries were optimized considering heat generation, equilibrium temperatures, and relative life. Two sets of curvatures were selected from the optimization: an inner-raceway curvature of 0.54, an outer-raceway curvature of 0.52, and an inner-raceway curvature of 0.55, an outer-raceway curvature of 0.53. A contact angle of 16° was also selected. Thermal gradients through the bearings were found to be lower with liquid lubrication than with solid film lubrication. As the coolant flowrate through the bearing increased, the ball temperature decreased but at a continuously decreasing rate. The optimum flowrate was approximately 4 kg/s. This paper describes the analytical modeling used to determine feasible modifications to improve bearing performance.

Introduction

The space shuttle main engine (SSME) high-pressure oxygen turbopump (HPOTP) bearings have shown heavy wear and significant deterioration after only 10 percent of their design service time (refs. 1 and 2). Bhat and Dolan (ref. 3) attribute the shortened bearing life to the large thermally induced internal loads and the high speeds at which the bearings run. Dufrane and Kannel (ref. 2) observed heavy wear, smearing, microcracking, and pitting with operating times of less than 6000 sec. After 100- to 4000-sec total operating time, surface oxide films have been observed on the rolling element and race surfaces, indicating high surface temperatures (ref. 1). In addition, ball paths with significant wear and/or plastic deformation were present at high contact angles, indicating the presence of high axial loads (ref. 1). To improve the performance of the HPOTP bearings, Dufrane and Kannel (ref. 1) recommend modifying the bearing clearances, the contact angle, and the outer-race clearances as well as improving cooling and lubrication.

A major cause of failure in high-speed ball bearings is excessive heat generation (ref. 4). The primary sources of heat generation in the bearings are the ball spinning friction in the ball-race contact areas, the rubbing friction between the cage and balls, and the cage locating surface on one of the races. Scibbe (ref. 4) emphasized that bearing lubrication should be sufficient to eliminate any race wear for several hours. To obtain minimum heat generation at high operating speeds, the bearing should be designed with small ball diameters and open race curvatures (ref. 5).

Much research has been accomplished in efforts to lower bearing friction and wear through different lubrication schemes. Brewe, Scibbe, and Wisander (ref. 6) evaluated seven self-lubricating ball-bearing retainer materials to determine their film transfer characteristics. This study showed that glass-fiber-filled polytetrafluoroethylene (PTFE) and bronze-filled PTFE retainers maintained a transfer film of PTFE on the inner-race tracks over extended periods of time.

Other studies (refs. 7 and 8) also demonstrated that retainers filled with PTFE maintained a transfer film. These studies showed that PTFE retainers are useful in cryogenic applications to reduce bearing friction. The HPOTP bearings presently incorporate a glass-fiber-filled PTFE retainer as a result of this previous work. However, this transfer-film method of solid lubrication provides only boundary lubrication, allowing wear to occur on the rolling elements and on the bearing races (ref. 9). Another approach has been liquid lubrication. However, it is difficult to find good lubricants that are liquid at cryogenic temperatures. A group of fluids that exhibit many of the lubricant properties required for cryogenic applications are the fluorinated polyethers. Studies (refs. 10 to 12) have shown that the operating characteristics of the fluorinated polyether fluids at cryogenic temperatures compare favorably with those of super-refined mineral oil at room temperature.

The objective of the work described in this paper was to analyze bearing performance through computer modeling of (1) variations in raceway curvatures and contact angles, (2) variations in the lubrication method, and (3) variations in the coolant flowrate.

The computer program SHABERTH was selected to analyze the bearing design, lubrication scheme, and cooling effects in an effort to improve bearing performance. SHABERTH can simulate thermomechanical performance of a load support

system for combinations of ball, cylindrical, and tapered roller bearings (ref. 13). Past studies have shown that SHABERTH can predict bearing temperatures and heat generation reasonably well (refs. 14 to 16). A model of the HPOTP bearing configuration was developed for SHABERTH. The bearing model was analyzed for both steady-state and transient conditions. All of the calculations were based on the assumption that low friction coefficients could be achieved. The results from this study compare heat generation, temperature, and life data for various configurations in an effort to determine a bearing design that can withstand the harsh conditions imposed on the HPOTP bearings.

Bearing Geometry

The cross section through the single bearing shown in figure 1 depicts the various diameters and radii associated with a ball bearing. A bearing is normally defined by its bore diameter d_b or its pitch diameter d_e. The pitch diameter equals the mean of the inner-raceway diameter d_i and the outer-raceway diameter d_o:

$$d_e = \frac{1}{2}(d_i + d_o) \tag{1}$$

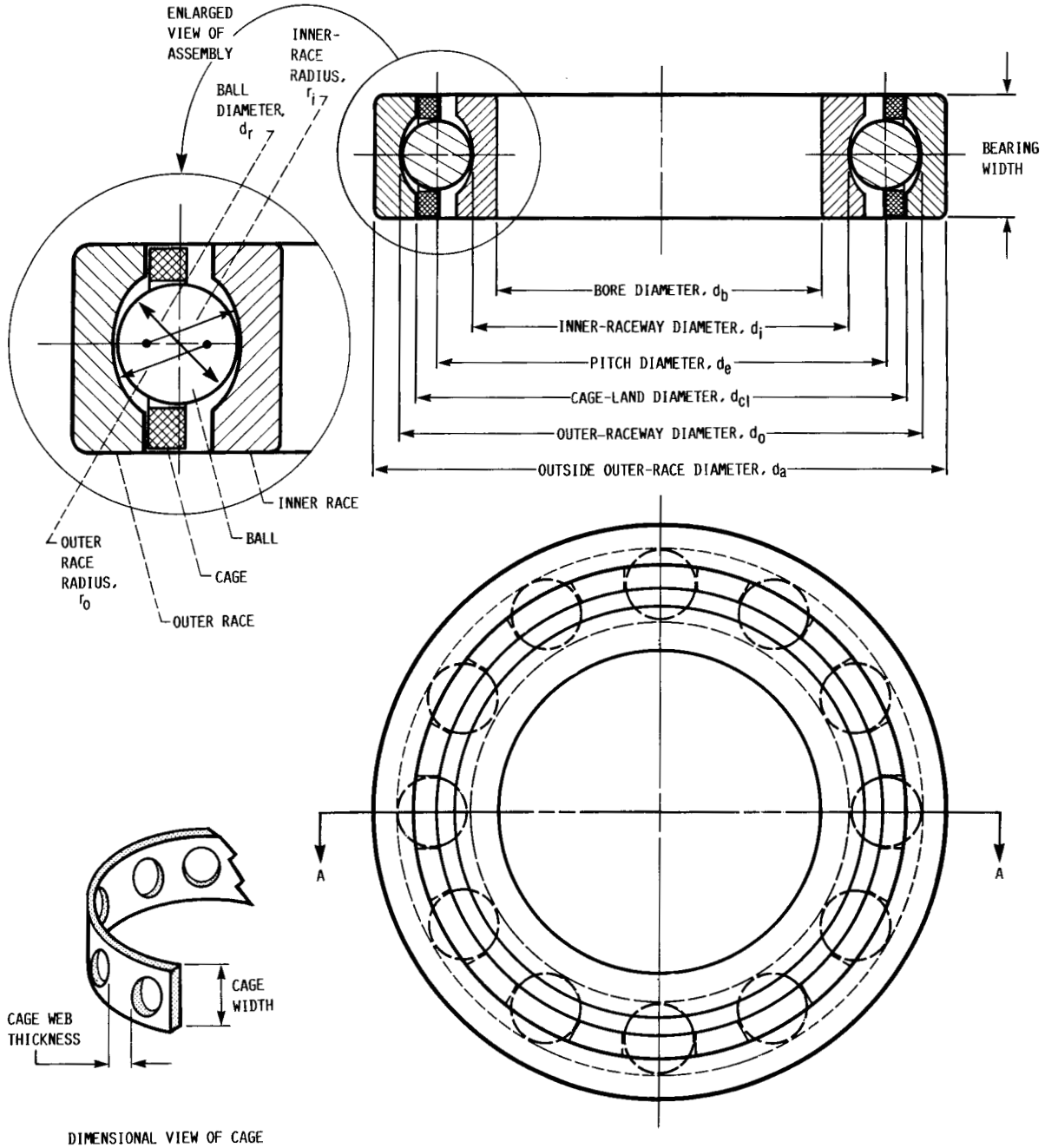

Figure 1.—Cross section of a single ball bearing.

The outside outer-race diameter is d_a, and the cage-land diameter is d_{cl}.

The inner-raceway curvature f_i and the outer-raceway curvature f_o are defined as

$$f_i = \frac{r_i}{d_r} \quad \text{and} \quad f_o = \frac{r_o}{d_r} \tag{2}$$

where r_i is the inner-race radius, r_o is the outer-race radius, and d_r is the diameter of the rolling element. Raceway curvature is a measure of the geometrical conformity of the race and the ball in a plane passing through the center of the bearing perpendicular to its plane and transverse to the race (ref. 17).

Because the bearing modifications must be retrofitted into the present bearing cavity, the bore diameter d_b, the outside outer-race diameter d_a, and the bearing width would not be changed. The type of bearing would remain an angular contact ball bearing. With these constraints, the other geometric parameters would also be limited to a range of values. The number of rolling elements must be sufficient for smooth operation, but limited so that the minimum allowable cage web thickness between the rolling elements is not compromised. The maximum size of the balls for the minimum allowable cage thickness is dependent on the number of balls. For a 57-mm-bore ball bearing with a d_a of 103 mm and a maximum cage width of 18.7 mm, the largest ball size is 15.9 mm diameter for 11 balls, 14.3 mm diameter for 12 balls, and 12.7 mm diameter for 13 balls. The three ball sizes were compared in a preliminary analysis using SHABERTH, and the thirteen 12.7-mm-diameter balls resulted in the lowest temperatures and the longest bearing life. Therefore, they were used in the rest of the analysis. It is accepted practice to use raceway curvatures (f_o and f_i) of 0.51 or greater. However, for curvatures above 0.60, there are increased contact stresses and decreased loading capacity, with diminishing returns in spin reduction (ref. 18). Since these curvatures are the suggested limits for turbopump applications, they were used as guidelines in this analysis.

Angular contact bearings are designed to operate under a combination of radial and thrust loads. The contact angle β for such a bearing (fig. 2) is defined as the angle made by a line through the points of contact of the ball and both races with a plane perpendicular to the bearing axis of rotation. With both a radial and thrust load, the contact angle of the balls when loaded cannot be zero. For the combined loads under consideration, a minimum effective mounted contact angle of 4° was used. The effective mounted contact angle is a function of the diametral clearance between the ball and the races for the mounted bearing at operating speeds and temperature, under no load. The maximum effective mounted contact angle used in this analysis was 28° because larger contact angles would result in a ball-race contact area at the edge of the race, according to contact area calculations using reference 17. The

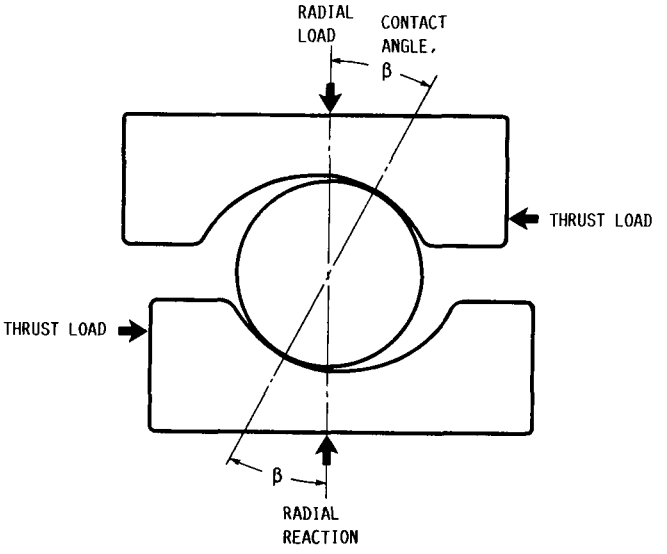

Figure 2.—Cross section of an angular contact ball bearing under static load conditions.

cage pocket clearance used was 1.00 mm, and the diametral clearance between the cage and the outer race was 1.02 mm.

In the HPOTP bearing, the coolant flowrate is dependent on how fast the oxygen moves through the turbopump and how effectively the oxygen can be pushed through the bearings. With the present bearing configuration, the coolant flows through the first bearing and then through the second bearing in series. Therefore, the coolant has a higher inlet temperature when it reaches the second bearing and cools it less effectively. A more effective means of cooling the bearings is to cool them in parallel with under-race cooling from separate cooling passages (ref. 19). The SHABERTH model uses separate cooling for each bearing for all analyses, and coolant conditions are changed only by varying the flowrate. For the oxygen-environment computer model of the HPOTP bearings, it was assumed that liquid oxygen was the coolant for all computations. It was further assumed that the heat transfer from the bearings would not change the liquid oxygen to gaseous oxygen and that liquid oxygen would flow through the bearings at all times, with either solid lubrication or liquid lubrication.

Shaberth Model

Computer Program

The SHABERTH computer program (ref. 13) used in this analysis was an upgraded version of an earlier SHABERTH developed for NASA Lewis Research Center (Crecelius, W.J.; Heller, S.; and Chiu, Y.P.: Improved Flexible Shaft-Bearing Thermal Analysis with NASA Friction Models and Cage Effects. SKF-AL-76P003, SKF Industries Inc., Feb. 1976). SHABERTH simulates the thermomechanical performance of a load support system consisting of a flexible shaft supported by up to five rolling element bearings. Any combination of

ball, cylindrical, or tapered roller bearings can be used to support the shaft. The applied loading can consist of point or distributed forces of moments and shaft misalignments. A lumped-mass thermal model allows calculation of steady-state or time-transient system temperatures considering free convection, forced convection, conduction, radiation, and mass transport heat transfer. A maximum of 100 temperature nodes can be used to describe the thermal system. The upgraded version includes modification of the cage model to calculate cage pocket and cage-land forces in the bearing and allows for a cage simulation, with single or multiple degrees of freedom, as well as allowing the program to analyze a single ball or roller bearing without the specifications of shaft geometry. A flowchart of the major capabilities of SHABERTH is shown in figure 3. The upgraded version used in the present analysis is described in detail in reference 13, which is a user's manual complete with program formulations, input instructions, and sample outputs.

To facilitate the present analysis, the program was changed to include an additional lubricant. SHABERTH uses preprogrammed lubricant properties for four specific lubricant types, or the user can specify no lubricant (dry friction). To specify any other lubricant types, the properties can be indicated in the input, and all unspecified properties are defaulted to the programmed properties. Since none of the preprogrammed lubricant types are remotely similar to the fluorinated

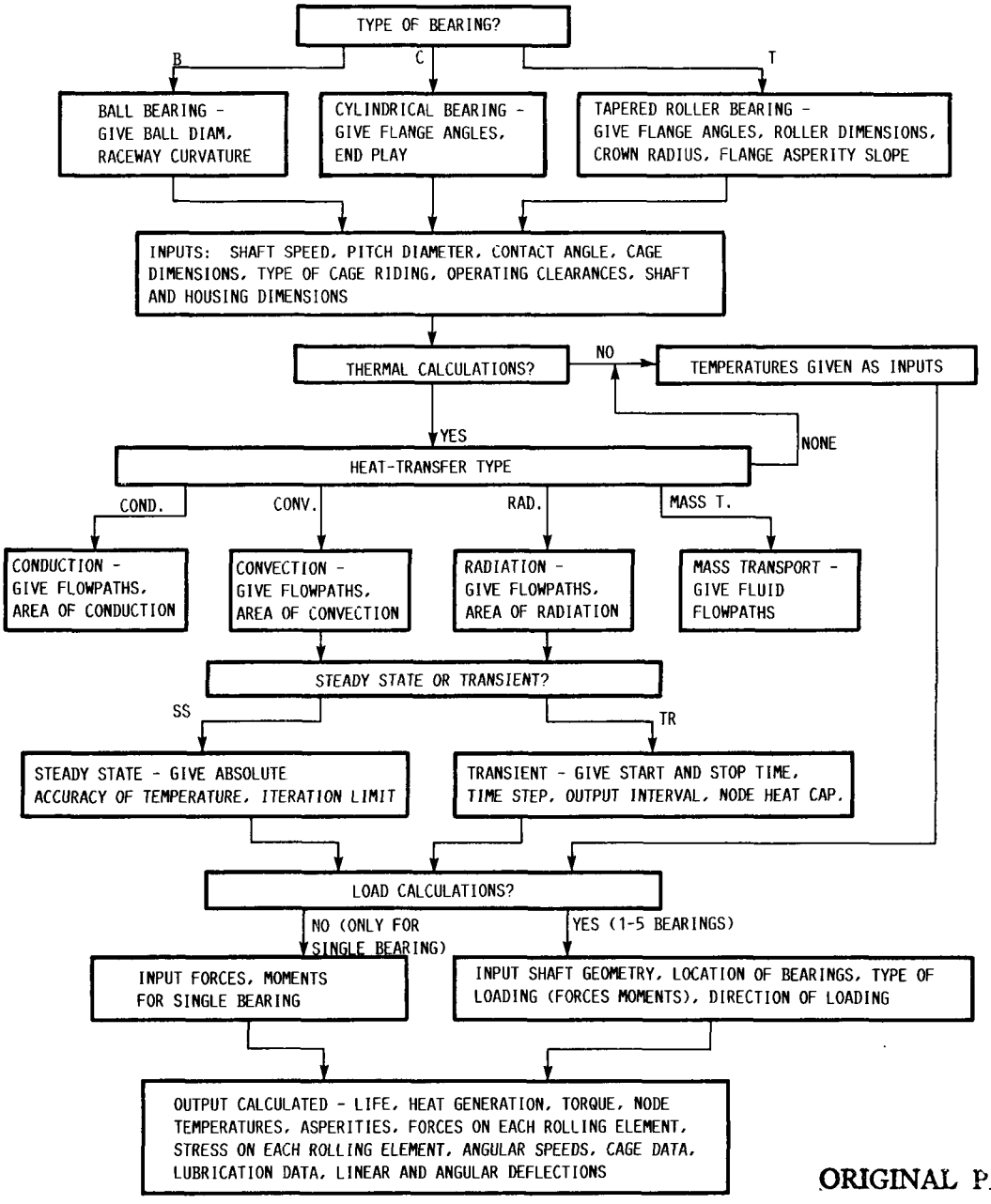

Figure 3.—Block diagram of SHABERTH capabilities.

polyethers used in the present analysis, the fluorinated polyether properties for Freon E-1 (ref. 20) were inserted in the program as a fifth lubricant type. These properties are shown in table I.

Bearing Simulation

The nodal system used on SHABERTH to model the 57-mm-bore ball bearing, shaft, and housing to be used in future testing is shown in figure 4. Because of symmetry, SHABERTH uses only the cross-sectional area from the shaft outward to the housing for analysis. In figure 4, nodes 1, 7, 12, and 13 are shaft nodes, nodes 2 to 5 and 8 to 11 are the bearing nodes (bearing nodes 3 and 9 are the balls, 4 and 10 are the cages, 2 and 8 are the inner races, and 5 and 11 are the outer races), nodes 6, 14, and 15 are the housing nodes, and nodes 16 to 18 are boundary nodes. These are all metal nodes. Node 19 is the air surrounding the bearing, nodes 20 to 23 are liquid oxygen (coolant) flowpaths, nodes 24 and 25 are the ambient air outside the boundaries, and node 26 is the liquid oxygen sump. Heat-transfer areas and conduction and convection paths were determined as suggested in the SHABERTH user's manual (ref. 13). Heat radiation was neglected in these calculations. Conduction paths exist between each metal node and all other metal nodes with which it has contact, between coolant nodes 20 and 22 and the bearing nodes (2 to 5 and 8 to 11), and between coolant node 21 and the shaft nodes (1, 7, 12, and 13). The path of the liquid oxygen coolant fluid flow is indicated by the dashed line in figure 4.

TABLE I.—FLUORINATED POLYETHER E-1 PROPERTIES AT ATMOSPHERIC PRESSURE[a]

	Temperature, K	
	200	298
Density, kg/m^3	1820	1540
Conductivity, w/m-°C	0.0839	0.0649
Specific heat, kJ/kg-°C	(b)	1.034
Dynamic viscosity, kg/m-s	4.0×10^{-3}	0.5×10^{-3}
Kinematic viscosity, m^2/s	2.2×10^{-6}	0.3×10^{-6}

[a]Reference 20.
[b]Not available in reference 20.

Results and Discussion

The space shuttle main engine (SSME) high-pressure oxygen turbopump (HPOTP) bearings have shown heavy wear and significant deterioration after only 10 percent of their design service time (refs. 1 and 2). Bhat and Dolan (ref. 3) attribute the shortened bearing life to the large, thermally induced

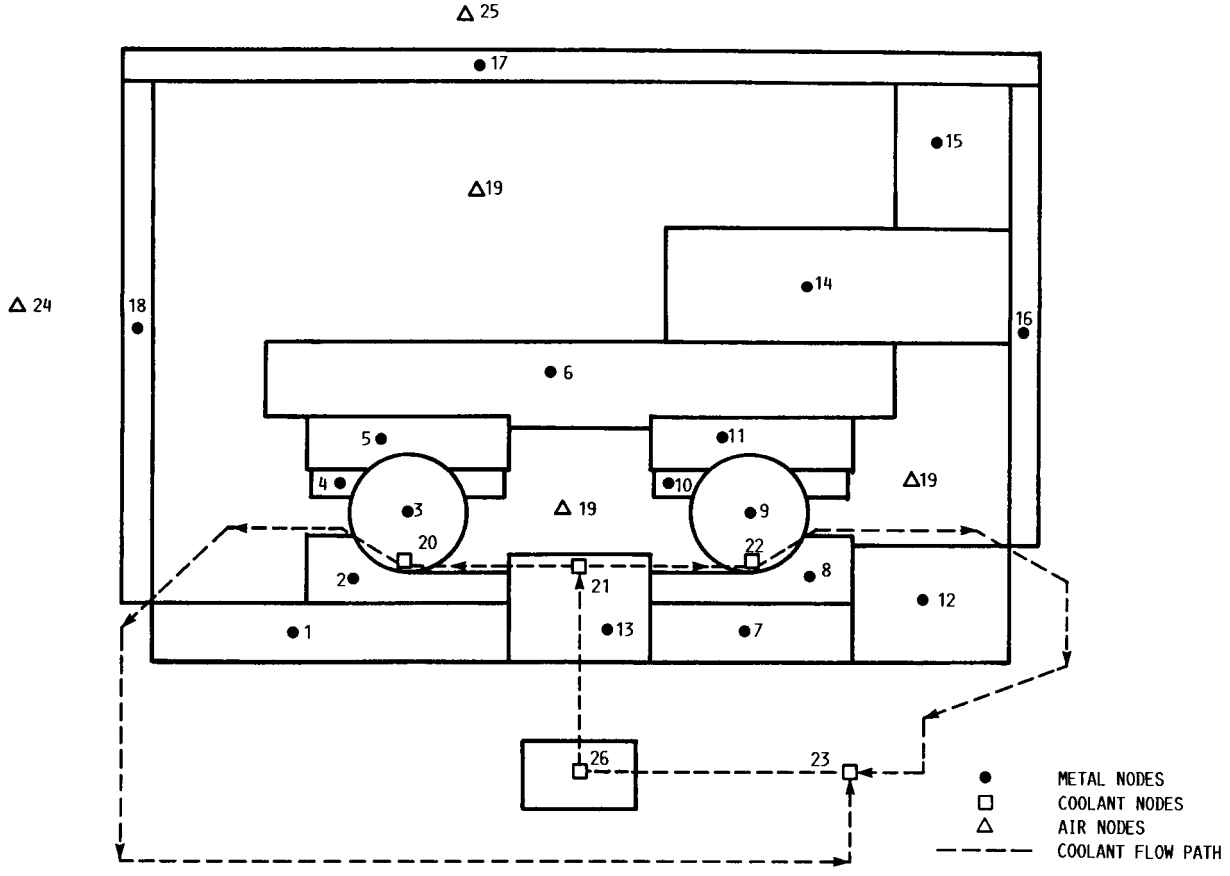

Figure 4.—Nodal system and coolant flow path used to model the 57-mm-bore bearing, shaft, and housing.

internal loads and the high speeds at which the bearings run. The computer program SHABERTH was used to calculate the performance of the HPOTP bearings. The bearing geometry and operating conditions that were varied included the raceway curvatures, the contact angle, the method of lubrication, and the coolant flowrate. The resulting rolling element fatigue life, temperature, and heat generation estimates were compared to determine performance for various operating conditions. To model the oxygen environment of the bearings, we gave all the bearing nodes initial temperatures of 90 K, the temperature of liquid oxygen at ambient pressure. Also, convective heat transfer coefficients were calculated by SHABERTH using oxygen properties (ref. 21) to determine the amount of heat transfer from the bearing nodes to the coolant nodes. It was assumed that liquid oxygen flows through the bearings for both solid and liquid lubrication cases.

Output Parameters

The primary output parameters discussed in this paper are fatigue life, temperature, and heat generation. SHABERTH calculates a bearing's L_{10} life, the time at which 10 percent of bearings under similar operating conditions would fail from rolling element (surface) fatigue. However, bearings seldom fail from rolling element fatigue: their failure is most often induced by improper installation, insufficient lubrication and cooling, or excessive loads. These conditions would fail a bearing before it fatigued. The life estimates in this paper are for fatigue life and, hence, are slightly optimistic. However, by comparing fatigue life estimates with various bearing parameters, trends in bearing life can be inferred. The temperature and heat generation estimates from SHABERTH have compared favorably with experimental results in past work (refs. 14 and 15).

Bearing Parameters

Many bearing parameters remained fixed throughout the study. These are summarized in table II. The diameters and widths correspond with the present HPOTP bearings. The analysis assumed a shaft speed of 30 000 rpm, an axial load of 4480 N, a radial load of 6720 N per bearing, and a liquid oxygen coolant flowrate of 0.45 kg/s, except for the coolant

TABLE II.—FIXED BEARING PARAMETERS[a]

Bore diameter, d_b, mm	57
Pitch diameter, d_e, mm	80.5
Cage-land diameter, d_{cl}, mm	86.9
Outside outer-race diameter, d_a, mm	103
Cage width, mm	18.7
Bearing width, mm	19.5
Shaft speed, rpm	30 000
Axial load, N	4480
Radial load, N	6720
Coolant flowrate[b], kg/s	0.45

[a]See figure 1.
[b]Not applicable to coolant flowrate analysis.

TABLE III.—OXYGEN PROPERTIES AT ATMOSPHERIC PRESSURE[a]

	Temperature, K	
	90	200
Density, kg/m^3	1140.9	1.955
Conductivity, w/m-°C	0.1516	0.01824
Specific heat, kJ/kg-°C	1.717	0.9131
Dynamic viscosity, m^2/s	1.196×10^{-3}	1.48×10^{-5}
Kinematic viscosity, kg/m-s	0.171×10^{-6}	7.59×10^{-6}

[a]Reference 21.

analysis. The calculated convective heat-transfer coefficients for the coolant used liquid oxygen properties (ref. 21), table III, and those for the liquid lubricant used Freon E-1 properties (ref. 20), table I. The bearing model had 13 balls (12.7 mm in diameter), the maximum number possible for this bearing configuration. The number of balls was maximized for the best distribution of load and for cage strength. The cage material was reinforced, glass-fiber-filled PTFE. The bearing material, for all parts except the cage, was vacuum-induction melted, vacuum-arc remelted (VIM-VAR) AISI 440C stainless steel. The material is compatible with an oxygen environment.

Geometry Optimization

The geometric parameters analyzed using SHABERTH include the raceway curvatures and the effective mounted contact angle. All geometry optimization calculations were run with liquid lubrication, Freon E-1, and liquid oxygen coolant. It was assumed that Freon E-1 was impregnated in the cage and that it lubricated the bearings. The liquid oxygen flow through the bearings was 0.45 kg/s for all geometry calculations. The raceway curvatures were varied for two effective mounted contact angles, 20° and 28°, to give an indication of trends when changing the raceway curvatures. Figure 5 shows the trends in life prediction as a function of inner-raceway curvature (f_i) for five outer-raceway curvatures (f_o). The raceway curvatures were varied from 0.52 to 0.58 in increments of 0.02. The present SSME bearing has an outer-raceway curvature of 0.53 and an inner-raceway curvature of 0.55. Figure 5(a) shows life prediction for an effective mounted contact angle of 20°, and figure 5(b) shows the life prediction for an effective mounted contact angle of 28°. Both figures demonstrate that longer life is achieved at smaller raceway curvatures.

Figure 6 shows the temperature trends as a function of inner-raceway curvature (f_i) for five outer-raceway curvatures (f_o). Figure 6(a) shows the estimated temperature of the balls for the various raceway curvatures with an effective mounted contact angle of 20°, and figure 6(b) shows the estimated ball temperature with an effective mounted contact angle of 28°. The trends on both figures indicate that a large inner-raceway

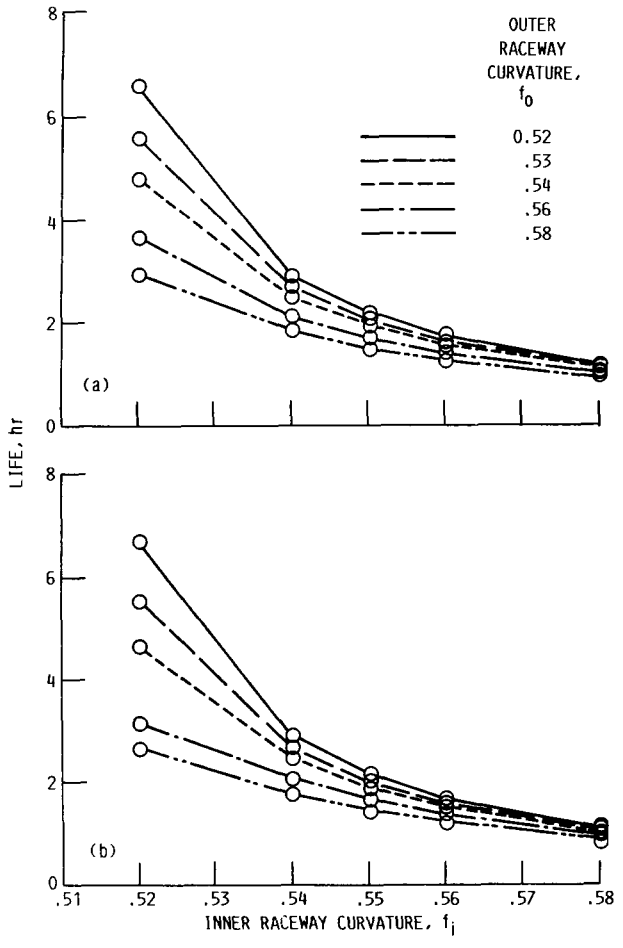

(a) Effective mounted contact angle, 20°.
(b) Effective mounted contact angle, 28°.

Figure 5.—Bearing fatigue life as a function of raceway curvature. Shaft speed, 30 000 rpm; thrust load, 4450 N; radial load, 6720 N per bearing; lubricant, Freon E-1; coolant flowrate, 0.45 kg/s.

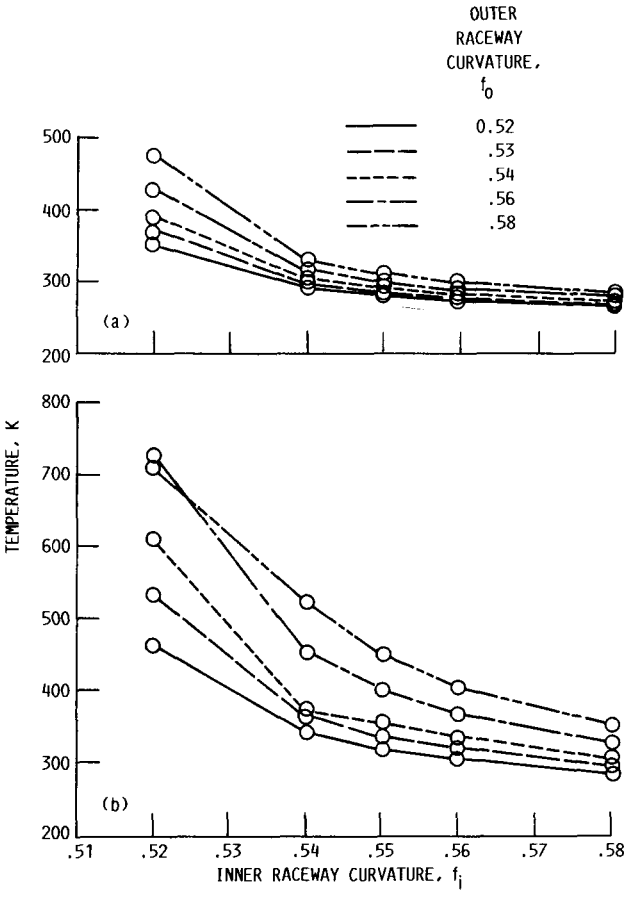

(a) Effective mounted contact angle, 20°.
(b) Effective mounted contact angle, 28°.

Figure 6.—Ball temperature as a function of raceway curvature. Shaft speed, 30 000 rpm; thrust load, 4450 N; radial load, 6720 N per bearing; lubricant, Freon E-1; coolant flowrate, 0.45 kg/s.

curvature results in low temperatures as do the small outer-raceway curvatures. Comparing the two figures demonstrates that smaller contact angles produce lower ball temperatures than larger contact angles.

The trends in heat generation for the bearings are shown in figure 7. Figure 7(a) shows the estimated total bearing heat generation for the various raceway curvatures with an effective mounted contact angle of 20°, and figure 7(b) shows the heat generated with an effective mounted contact angle of 28°. As with the trends in temperature, the larger inner-raceway curvatures result in less generated heat as do the smaller outer-raceway curvatures. Comparing figure 7(a) with 7(b) indicates that the smaller contact angle generates less heat than the larger contact angle.

Bearing fatigue life is dependent on the hertzian stresses, but bearing temperature is dependent on the amount of generated heat. As the raceway curvature increases, there is less contact area between the ball and the raceway. The smaller contact area lowers the amount of generated heat but raises the amount of stress (with load constant and a decrease in area).

Figures 6 and 7 indicate, however, that smaller outer-raceway curvatures generate less heat than larger outer-raceway curvatures. For bearings with large bore diameters (above 50 mm) and high speed, the outer-raceway curvature is normally less than the inner-raceway curvature. This reduces the heat generation from ball spinning at the inner-race contact (ref. 18). The data in figures 5 to 7 indicate that medium range inner-raceway curvatures (0.54 to 0.55) combine the benefits of low heat generation at large curvatures and long life at small curvatures. Low outer-raceway curvatures (0.52 to 0.53) were selected because they result in longer life, lower temperatures, and lower heat generation for the bearings. From these results, two sets of curvatures were selected for use when selecting the contact angle: $f_o = 0.52$, $f_i = 0.54$, and $f_o = 0.53$, $f_i = 0.55$. Another set of curvatures, $f_o = 0.54$, $f_i = 0.58$, was chosen for comparison.

Figure 8 shows the estimated fatigue life as a function of effective mounted contact angle for the three sets of curvatures. The estimated life for a particular set of curvatures increases up to a contact angle of 16° and then remains fairly constant.

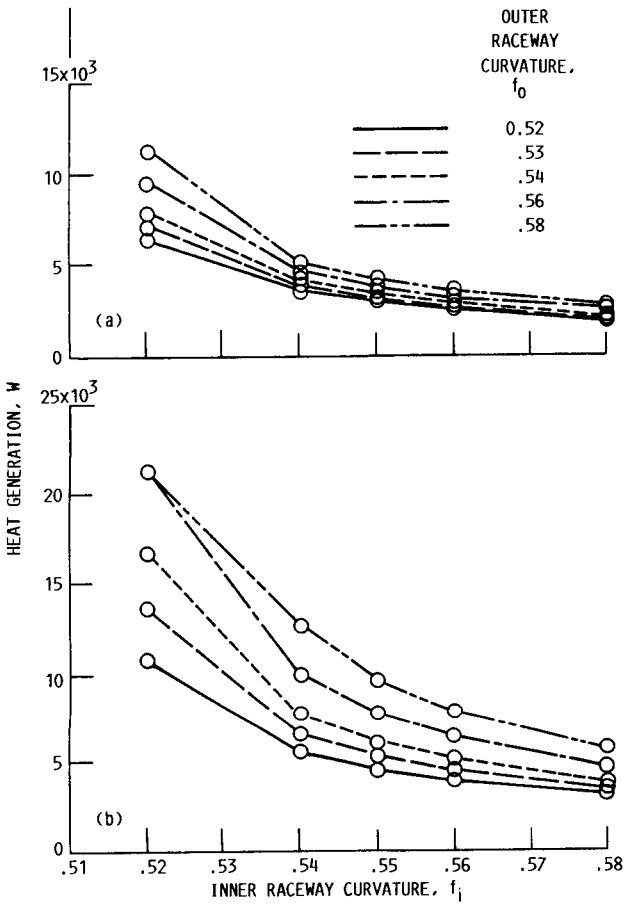

(a) Effective mounted contact angle, 20°.
(b) Effective mounted contact angle, 28°.

Figure 7.—Total bearing heat generation as a function of raceway curvature. Shaft speed, 30 000 rpm; thrust load, 4450 N; radial load, 6720 N per bearing; lubricant, Freon E-1; coolant flowrate, 0.45 kg/s.

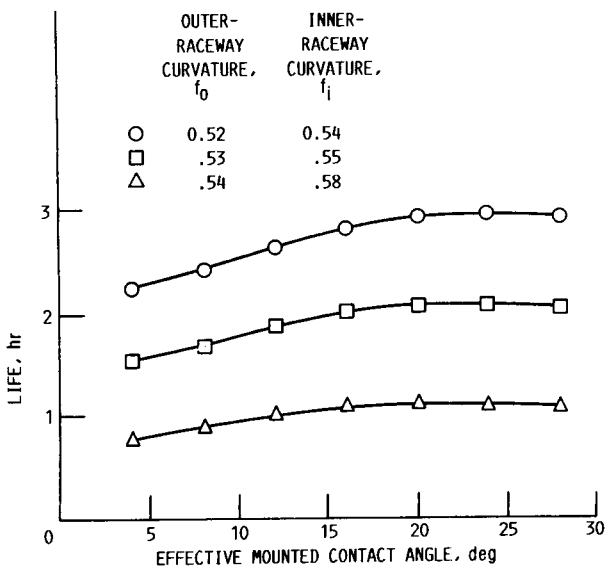

Figure 8.—Bearing fatigue life as a function of effective mounted contact angle. Shaft speed, 30 000 rpm; thrust load, 4450 N; radial load, 6720 N per bearing; lubricant, Freon E-1; coolant flowrate, 0.45 kg/s.

The ball temperatures for various contact angles are shown in figure 9. As the contact angle increases, the ball temperature increases at an increasing rate.

The heat generated in the bearing for various contact angles is shown in figure 10. The heat generation results follow the same trend as those of the temperature, with the effect of the increase in heat generation becoming greater with increasing contact angle.

From figures 8, 9, and 10, an effective mounted contact angle between 8° and 16 ° would give the best bearing performance. For maximum load capacity and minimum torque, Butner (ref. 18) suggests that the contact angle be greater than 12° to 15°. Therefore, a contact angle of 16° was chosen for the preferred design.

The subsequent analyses implement the geometry configurations chosen in the geometry optimization portion of the study. Two sets of curvatures were used: $f_o = 0.52$, $f_i = 0.54$, and $f_o = 0.53$, $f_i = 0.55$. These were selected in

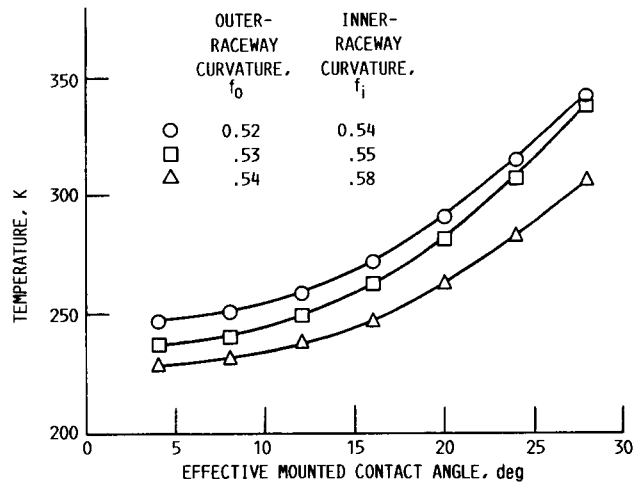

Figure 9.—Ball temperature as a function of effective mounted contact angle. Shaft speed, 30 000 rpm; thrust load, 4450 N; radial load, 6720 N per bearing; lubricant, Freon E-1; coolant flowrate, 0.45 kg/s.

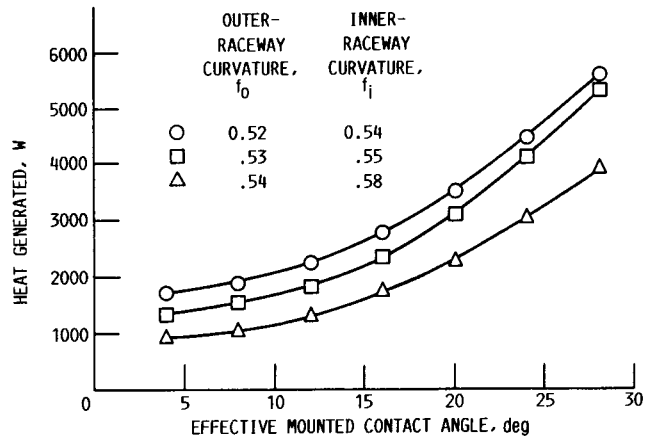

Figure 10.—Total bearing heat generation as a function of effective mounted contact angle. Shaft speed, 30 000 rpm; thrust load, 4450 N; radial load, 6720 N per bearing; lubricant, Freon E-1, coolant flowrate, 0.45 kg/s.

the raceway curvature analysis. The contact angles selected were 16° and 22°. The 16° angle was selected in the contact angle analysis, and 22° is the operating contact angle of the present HPOTP bearings.

Lubrication

After determining geometry configurations for the best performance, the type of lubricant was analyzed. Most lubricants are incompatible with liquid oxygen and/or are ineffective at cryogenic temperatures (refs. 4, 5, and 10). However, there are several possible lubricants, including liquid fluorinated polyethers (ref. 12) and certain solids (refs. 5 and 6). For the fluorinated polyethers, fluid properties (ref. 20) were written into the software so that they could be used for future work as well as in the present work. The fluorinated polyether used for this analysis was Freon E-1. Table I gives the properties for this lubricant.

Solid film lubrication coats the balls and/or raceways with a solid film that has a lower coefficient of friction than the bearing material. Possible coatings include gold, silver, lead, and PTFE. Gold, silver, and lead coatings are applied directly to the bearing before operation, while PTFE coatings normally are the result of a film transferred from a PTFE retainer to the ball. Lead coatings can also be applied in this manner (ref. 22). In SHABERTH, the solid film lubricant was modeled as dry friction with a ball-race friction coefficient reflecting the use of a coating. The friction coefficients used in this analysis were for PTFE rubbing steel. All solid film lubrication computations were calculated with liquid oxygen coolant flow.

For the transient analysis, computations were made every 0.1 sec and bearing temperatures were printed for every 1.0 sec. It was assumed that the shaft speed reaches 30 000 rpm instantaneously (within the first 0.1 sec). The analyses only include the first 30 sec of operation because steady state was reached in all cases in that time period.

The results of the transient thermal analysis of the bearing operation for both types of lubrication is shown in figures 11 and 12. In most cases, the final, equilibrium temperature was reached in about 5 sec. The operating conditions for figures 11 and 12 are given in table II. Since the properties of the liquid lubricant, Freon E-1, were outside the range of validity of the equations in SHABERTH below 200 K, the liquid lubricated cases were run on SHABERTH with an initial temperature of 200 K. In actual testing, it would be assumed that the liquid lubricated bearings would run with dry friction from the initial temperature of 90 K, the temperature of liquid oxygen at ambient pressure, until the lubricant began to melt. Then, the bearings would run lubricated. However, with solid film lubrication the bearings were run on SHABERTH with the coatings from the initial temperature of 90 K, which can be accurately modeled with SHABERTH.

Figures 11(a) and (b) show bearing temperatures for an f_o of 0.52, and f_i of 0.54, and an effective mounted contact angle of 16°. With liquid lubrication (fig. 11(a)), the thermal

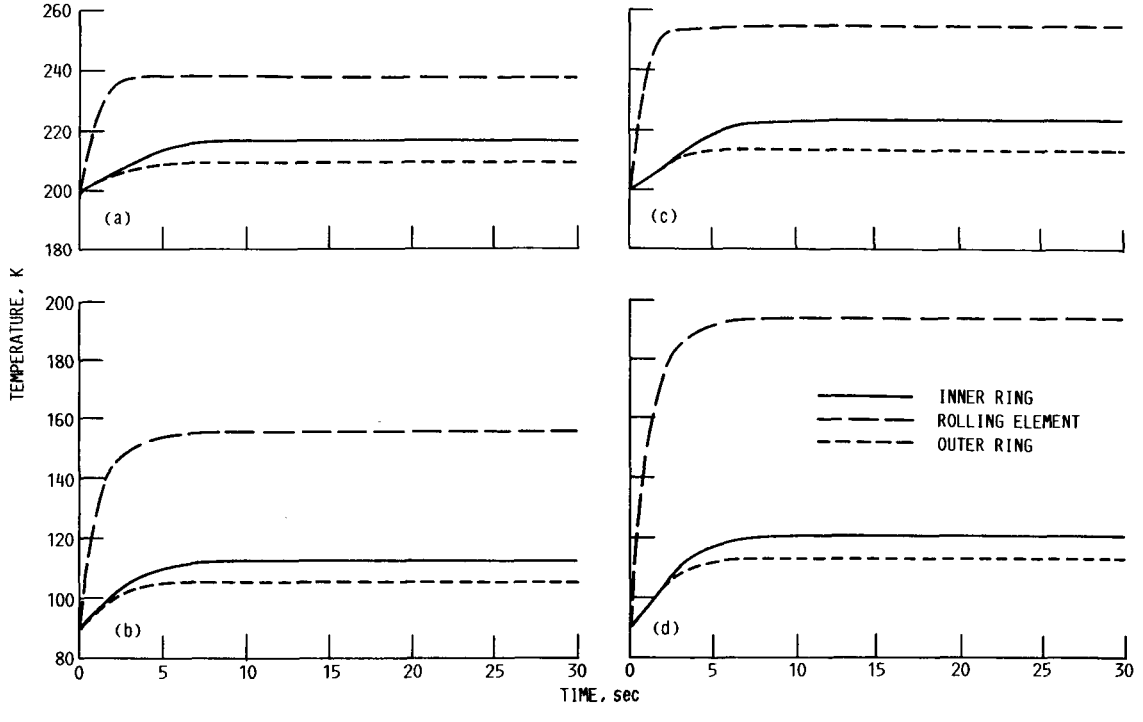

(a) Liquid lubrication, Freon E-1; contact angle 16°.
(b) Solid lubrication, PTFE; contact angle, 16°.
(c) Liquid lubrication, Freon E-1; contact angle, 22°.
(d) Solid lubrication, PTFE; contact angle, 22°.

Figure 11.—Bearing temperature as a function of time for an outer-raceway curvature of 0.52 and an inner-raceway curvature of 0.54. Shaft speed, 30 000 rpm; thrust load, 4450 N; radial load, 6720 N per bearing; coolant flowrate, 0.45 kg/s.

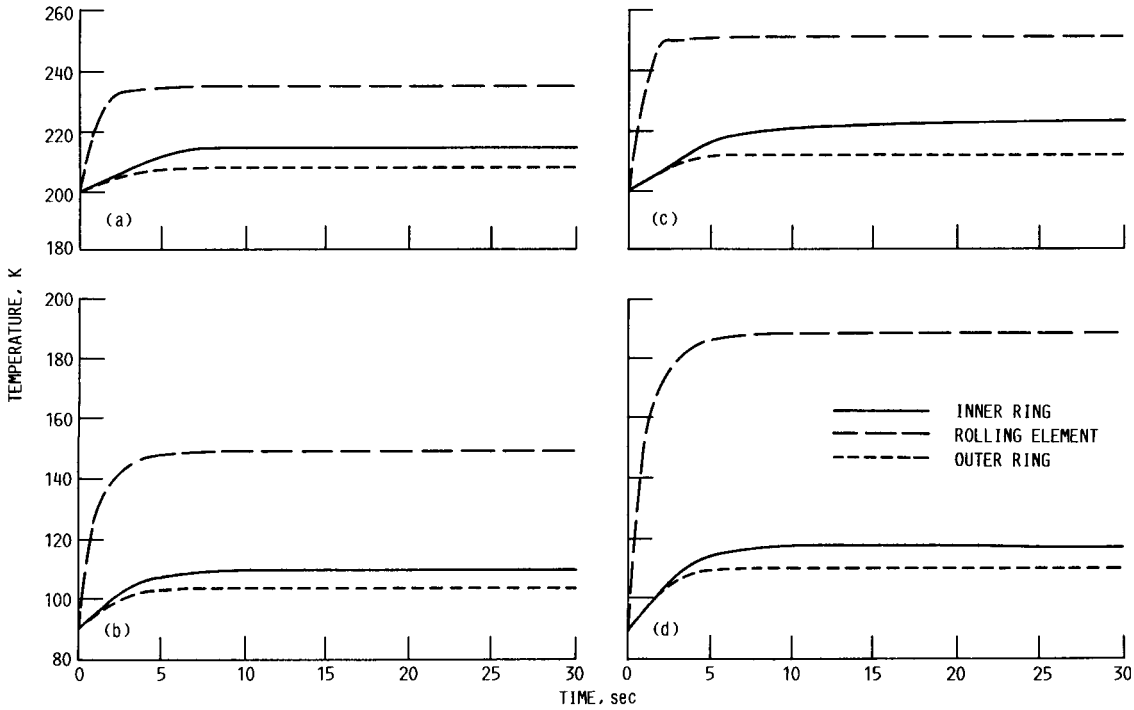

(a) Liquid lubrication, Freon E-1; contact angle, 16°.
(b) Solid lubrication, PTFE; contact angle, 16°.
(c) Liquid lubrication, Freon E-1; contact angle, 22°.
(d) Solid lubrication, PTFE; contact angle, 22°.

Figure 12.—Bearing temperature as a function of time for an outer-raceway curvature of 0.53 and an inner-raceway curvature of 0.55. Shaft speed, 30 000 rpm; thrust load, 4450 N; radial load, 6720 N per bearing; coolant flowrate, 0.45 kg/s.

gradient between the ball and the inner race is 21 K and the thermal gradient between the ball and the outer race is 28 K. With solid film lubrication (fig. 11(b)), the thermal gradient between the ball and the inner race is 43 K and the thermal gradient between the ball and the outer race is 50 K. The thermal gradient through the bearing with liquid lubrication is 22 K less than with solid film lubrication.

Changing the effective mounted contact angle from 16° to 22° yielded a large rise in thermal gradients, as can be seen in figures 11(c) and (d). Figure 11(c) shows the thermal gradients for liquid lubrication. The difference in temperature between the ball and the inner race is 31 K and between the ball and the outer race is 40 K. In figure 11(d) temperatures for solid film lubrication are shown. The difference in temperature between the ball and the inner race is 72 K and between the ball and the outer race is 80 K. These gradients are much larger than with the smaller effective mounted contact angle of 16°.

Figures 12(a) and (b) show bearing temperatures for an f_o of 0.53, an f_i of 0.55, and an effective mounted contact angle of 16°. With liquid lubrication, thermal gradients of 20 and 27 K result between the ball and the inner race and between the ball and the outer race, respectively (fig. 12(a)). With solid-film lubrication, thermal gradients of 39 and 45 K result between the ball and the inner race and between the ball and the outer race, respectively (fig. 12(b)).

Bearing temperatures for an f_o of 0.53, and f_i of 0.55, and an effective mounted contact angle of 22° are shown in figures 12(c) and (d). For liquid lubrication (fig. 12(c)), the difference in temperature between the ball and the inner race is 31 K and between the ball and the outer race is 41 K. For solid film lubrication (fig. 12(d)), the difference in temperature between the ball and the inner race is 70 K and between the ball and the outer race is 78 K. These gradients are consistent with figures 12(a) and (b).

These figures, which are based on SHABERTH calculations, indicate that thermal gradients through the bearing at the ball-race contact are lower with liquid lubrication than with solid film lubrication.

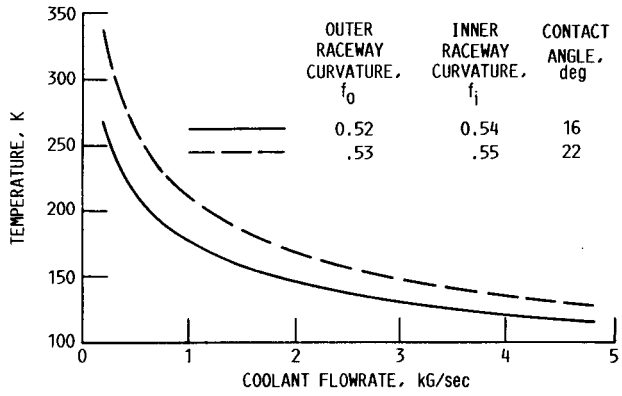

Figure 13.—Ball temperature as a function of coolant flowrate. Shaft speed, 30 000 rpm; thrust load, 4450 N; radial load, 6720 N per bearing; lubricant, PTFE.

Coolant Flowrate

The flowrate was varied from 0.2 to 4.5 kg/s to determine the effect of coolant flowrate on the bearings. In figure 13, the ball temperature is shown as a function of the coolant flowrate for two geometry configurations. The flowrates are the flow through one of the bearings. As can be seen, the temperature decreases as the flowrate increases, but at a decreasing rate. From figure 13, the optimum flowrate would be approximately 4 kg/s because of diminishing returns in temperature for larger flows.

Summary of Results

The bearings presently used in the high-pressure oxygen turbopump (HPOTP) of the space shuttle main engine (SSME) have a relatively short life because of the large thermally induced internal loads and the high speeds imposed upon the system. An analysis was performed to determine how these internal loads can be minimized and how the detrimental effect of the high speeds can be reduced. Several parameters can be changed in the bearing configuration for improved performance of the ball bearing. The computer program SHABERTH was selected to analyze several of these parameters: the curvature of the races, the contact angle, the coolant flowrate, and the method of lubrication. A model of the 57-mm-bore ball bearing, shaft, and housing to be used in a proposed experimental test effort was analyzed for both steady-state and transient conditions. All calculations were based on an assumption that low friction coefficients could be achieved whether solid film or liquid lubrication was used. It was assumed for all computations that liquid oxygen cooled the bearings. The results from this analysis compared heat generation, temperature, and fatigue life predictions for various configurations in an effort to determine a bearing design that can withstand the harsh conditions imposed on the HPOTP bearings. The following results were obtained:

1. Bearing geometries to be tested in a proposed experimental effort were optimized considering heat generation, equilibrium temperatures, and relative life. Outer-raceway curvatures f_o of 0.52 to 0.53 were selected because they result in long life, low temperatures, and low heat generation for the bearings. Inner-raceway curvatures f_i of 0.54 to 0.55 were selected because they combine the benefits of low heat generation at large inner-raceway curvatures and long life at small inner-raceway curvatures. Therefore, two sets of curvatures were selected from the optimization: $f_i = 0.54$, $f_o = 0.52$, and $f_i = 0.55$, $f_o = 0.53$. An effective mounted contact angle of 16° was selected for maximum load capacity and minimum torque. Smaller contact angles result in shorter life while larger contact angles result in more heat generation and higher temperatures.

2. Thermal gradients through the bearing are less with liquid lubrication than with solid film lubrication. Also, the temperature gradient through the bearing increases with increasing effective mounted contact angle.

3. As the coolant flowrate through the bearing increases, the ball temperature decreases at a decreasing rate. The optimum flowrate would be approximately 4 kg/s because of the diminishing returns in temperature for larger flows.

Lewis Research Center
National Aeronautics and Space Administration
Cleveland, Ohio, January 4, 1988

References

1. Dufrane, K.F.; and Kannel, J.W.: Evaluation of SSME HPOTP Bearings from Units 2023, 2024, 6002. Battelle Columbus Labs, OH, Feb. 27, 1987.
2. Dufrane, K.F.; and Kannel, J.W.: Evaluation of Space Shuttle Main Engine Bearings from High Pressure Oxygen Turbopump 9008. NASA CR-161516, 1980.
3. Bhat, B.N.; and Dolan, F.J.: Past Performance Analysis of HPOTP Bearings. NASA TM-82470, 1982.
4. Scibbe, H.W.: Bearings and Seals for Cryogenic Fluids. SAE paper 680550, Oct. 1967. (NASA TM X-52415.)
5. Scibbe, H.W.; Brewe, D.E.; and Coe, H.H.: Lubrication and Wear of Ball Bearings in Cryogenic Hydrogen. NASA TM X-52476, 1968.
6. Brewe, D.E.; Scibbe, H.W.; and Anderson, W.J.: Film-Transfer Studies of Seven Ball-Bearing Retainer Materials in 60 °R (33 °K) Hydrogen Gas at 0.8 Million DN Value. NASA TN D-3730, 1966.
7. Wisander, D.W.; Ludwig, L.C.; and Johnson, R.L.: Wear and Friction of Various Polymer Laminates in Liquid Nitrogen and in Liquid Hydrogen. NASA TN D-3706, 1966.
8. Zaretsky, E.V.; Scibbe, W.W.; and Brewe, D.E.: Studies of Low and High Temperature Cage Materials. Bearing and Seal Design in Nuclear Power Machinery, R.A. Burton, ed., ASME, 1967, pp. 33-51. (NASA TM X-52262.)
9. Brewe, D.E.; Coe, H.H.; and Scibbe, H.W.: Cooling Studies with High Speed Ball Bearings Operating in Cold Hydrogen Gas. ASLE Trans., vol. 12, 1969, pp. 66-76.
10. Dietrich, M.W.; Townsend, D.P.; and Zaretsky, E.V.: Rolling-Element Lubrication with Fluorinated Polyether at Cryogenic Temperatures (160° to 410 °R). NASA TN D-5566, 1969.
11. Dietrich, M.W.; Townsend, D.P.; and Zaretsky, E.V.: Rolling Element Fatigue and Lubrication with Fluorinated Polyethers at Cryogenic Temperatures. ASME Paper 70-LUB-17, Oct. 1970. (NASA TM X-52863.)
12. Dietrich, M.W.; and Zaretsky, E.V.: Effect of Viscosity on Rolling Element Fatigue Life at Cryogenic Temperatures with Fluorinated Ether Lubricants. NASA TN D-7953, 1975.
13. Hadden, G.B., et al: Research Report—User's Manual for Computer Program AT81Y003 SHABERTH. Steady State and Transient Thermal Analysis of a Shaft Bearing System Including Ball, Cylindrical, and Tapered Roller Bearings. (SKF-AT81D040, SKF Technology Services; NASA Contract NAS3-22690) NASA CR-165365, 1981.
14. Coe, H.H.; and Zaretsky. E.V.: Predicted and Experimental Performance of Jet-Lubricated 120-Millimeter-Bore Ball Bearings Operating to 2.5 Million DN. NASA TP-1196, 1978.
15. Parker, R.J.: Comparison of Predicted and Experimental Thermal Performance of Angular Contact Ball Bearings. NASA TP-2275, 1984.
16. Maurer, R.E.; and Pallini, R.A.: Computer-Aided Selection of Materials for Cryogenic Turbopump Bearings. Lubr. Eng., vol. 42, no. 2, 1986, pp. 78-83.

17. Hamrock, B.J.; and Anderson. W.J.: Rolling-Element Bearings. NASA RP-1105, 1983.
18. Butner, M.F.; and Keller, R.B., Jr.: Liquid Rocket Engine Turbopump Bearings. NASA SP-8048, 1971.
19. Zaretsky, E.V.; Schuller, F.T.; and Coe, H.H.: Lubrication and Performance of High Speed Rolling-Element Bearings. Lubr. Eng., vol. 41, no. 10, Oct. 1985, pp. 725–732. (NASA TM–86958.)
20. FREON E Series Fluorocarbons. Dupont Technologies Bulletin EL–8B, 1967.
21. Roder, H.M.; and Weber, L.A.: ASRDI Oxygen Technology Survey. Volume I: Thermophysical Properties. NASA SP-3071, 1972.
22. Wisander, D.W.; Brewe, D.E.; and Scibbe, H.W.: Performance of High Speed Ball Bearings with Lead-Plated Retainers in Liquid Hydrogen for Potential Use in a Radiation Environment. NASA TN D–6653, 1972.

NASA
National Aeronautics and Space Administration

Report Documentation Page

1. Report No.	2. Government Accession No.	3. Recipient's Catalog No.
NASA TP-2816		

4. Title and Subtitle
Computer-Aided Design Analysis of 57-mm, Angular-Contact, Cryogenic Turbopump Bearings

5. Report Date
March 1988

6. Performing Organization Code

7. Author(s)
Elizabeth S. Armstrong and Harold H. Coe

8. Performing Organization Report No.
E-3890

10. Work Unit No.
582-01-11

9. Performing Organization Name and Address
National Aeronautics and Space Administration
Lewis Research Center
Cleveland, Ohio 44135-3191

11. Contract or Grant No.

13. Type of Report and Period Covered
Technical Paper

12. Sponsoring Agency Name and Address
National Aeronautics and Space Administration
Washington, D.C. 20546-0001

14. Sponsoring Agency Code

15. Supplementary Notes

16. Abstract

The space shuttle main engine (SSME) high-pressure oxygen turbopumps (HPOTP) have not experienced the service life required of them. This insufficiency has been due in part to the shortened life of the bearings. To improve the life of the existing turbopump bearings, an effort is being undertaken to investigate bearing modifications that could be retrofitted into the present bearing cavity. Several bearing parameters were optimized using the computer program SHABERTH, which performs a thermomechanical simulation of a load support system. The computer analysis showed that improved bearing performance is feasible if low friction coefficients can be attained. Bearing geometries were optimized considering heat generation, equilibrium temperatures, and relative life. Thermal gradients through the bearings were found to be lower with liquid lubrication than with solid film lubrication and a liquid oxygen coolant flowrate of approximately 4.0 kg/s was found to be optimum. This paper describes the analytical modeling used to determine these feasible modifications to improve bearing performance.

17. Key Words (Suggested by Author(s))	18. Distribution Statement
Cryogenic bearings; Ball bearings; Liquid oxygen; Turbine pumps; Thermal analysis; Space shuttle main engine; Bearings	Unclassified – Unlimited Subject Category 37

19. Security Classif. (of this report)	20. Security Classif. (of this page)	21. No of pages	22. Price*
Unclassified	Unclassified	14	A02

NASA FORM 1626 OCT 86

*For sale by the National Technical Information Service, Springfield, Virginia 22161

NASA-Langley, 1988